FEATURE ARTICLE

Journal of Materials Chemistry
www.rsc.org/materials

Scanning probe microscopies beyond imaging†

Paolo Samorì[a,b]

[a]*Istituto per la Sintesi Organica e la Fotoreattività- Consiglio Nazionale delle Ricerche, via Gobetti 101, 40129 Bologna, Italy. E-mail: samori@isof.cnr.it*
[b]*Institut de Science et d'Ingénierie Supramoléculaires (I.S.I.S.)-Université Louis Pasteur 8, allée Gaspard Monge, BP 70028, F-67083 Strasbourg Cedex, France*

Received 14th November 2003, Accepted 6th January 2004
First published as an Advance Article on the web 1st March 2004

Unraveling physico-chemical properties of molecule based architectures across a wide range of length scales represents one of the major goals of materials science. Scanning Probe Microscopies (SPMs) permit not only the imaging of surfaces, but most interestingly they also make it possible to gain insight into a variety of physical and chemical properties of molecule-based structures occurring in scales ranging from the hundreds of micrometers down to the sub-nanometer regime. Moreover they allow the manipulation of objects with a nanoscale precision, thereby making it possible to nanopattern a surface or to cast light onto the nanomechanics of complex assemblies. Thus, they can provide crucial information for the optimisation of functional materials. This Feature article reviews recent progress in the use of SPMs beyond imaging on soft materials, with a particular emphasis on the chemical discrimination, mechanical properties of macromolecules, tip induced reactions and manipulations as well as on the study of electrical properties of materials on the nanoscale.

Paolo Samorì, born in Imola (Italy) in 1971, obtained his Laurea in Industrial Chemistry at the University of Bologna. Then, he joined the group of Prof. J. P. Rabe at the Humboldt University Berlin (Germany), where he received his doctorate in 2000 for work on the self-assembly of π-conjugated (macro)molecules at surfaces and interfaces. After a Post Doc in the group of Prof. J. P. Rabe he was appointed, in 2001, Researcher at the Institute for the Organic Synthesis and Photoreactivity of the National Research Council (Italy). From 2003 he was invited to hold a Visiting Professorship at the Institut de Science et d'Ingénierie Supramoléculaires (I.S.I.S.)-Universitè Louis Pasteur of Strasbourg (France). His current research interests include the self-assembly of hybrid architectures at surfaces, supramolecular electronics and the fabrication of molecular scale nanodevices. His work has been awarded various prizes including the graduate student awards at EMRS (in 1998) and MRS (2000) as well as the IUPAC Prize for Young Chemists 2001.

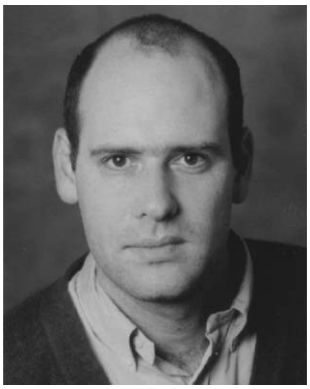

Paolo Samorì

Introduction

Nanoscale science and nanotechnology are cross-disciplinary areas involving functional systems and materials whose structures and components, due to their nanoscale size, possess unusual or enhanced properties. The processing and the manipulation of complex architectures on the nanoscale as well as the fabrication of devices with new sustainable approaches are key issues towards a technology based on smart materials. The invention of Scanning Tunnelling Microscopy (STM) in 1982 by Gerd Binnig and Heinrich Rohrer represented a true breakthrough in nanoscale science and nanotechnology.[1–3] STM allowed for the first time to produce real-space images of electrically conductive surfaces with sub-nanometre scale resolution. The development of the Atomic Force Microscope (AFM), known also as the Scanning Force Microscope (SFM),[4–7] permitted the extension of explorations to electrically insulating materials such as biomolecules and polymers. A major advantage of Scanning Probe Microscopies (SPMs) is that they can operate under different media such as air, liquid, and gas streams, expanding in this way the studies to environments that are technologically more important and also more easily accessible and less expensive than ultra-high vacuum (UHV). As a consequence, they allow visualisation of amorphous or crystalline structures of organic adsorbates,[8] including porous materials.[9] Moreover, they allow monitoring of dynamic phenomena such as chemical reactions[10,11] as well as the diffusional path of single molecules,[12] the healing of a crystalline surface of alkanethiols self-assembled on metallic surfaces,[13] and the process of crystallisation.[14] Exploiting these microscopies, one can attain a spatial resolution along the *X*-, *Y*-, and *Z*-directions of a fraction of an ångström. The techniques basically convey a sharp probe (tip) that interacts locally with a sample surface during raster scanning. The SPMs differ as regards to the prime physical property that is measured and employed to analyse the surface.

After a first period when these methodologies have been primarily utilized for creating nice pictures of surfaces, the implementation of new modes of scanning and new SPMs paved the way towards their use to bestow information on the physico-chemical properties of the matter and on inducing actions that can single-out characteristics of the molecular system investigated. In this Feature article the most important results obtained exploiting SPM beyond imaging, in particular using STM and SFM based set-ups, will be highlighted. Due to the extremely large number of works performed with these methods in many scientific disciplines and on a variety of materials, spanning from supramolecular materials, to biological systems, to classical semiconductors, *etc.*, this paper will mainly focus on (bio)organic-systems and I will not extensively

† Dedicated to Prof. Frans C. De Schryver on the occasion of his 65th birthday.

DOI: 10.1039/b314626j

treat every achievement. This article is divided into the following four main chapters:

(1) Study of the chemical discrimination, by STM and Chemical Force Microscopy;

(2) Investigation of the mechanical properties of macromolecules, with SFM imaging and Force Spectroscopy;

(3) Nanomanipulations by STM and SFM based approaches;

(4) Determination of electrical properties of ordered architectures, using STM and SFM based set-ups.

Chemical discrimination

STM monitoring of the local density of state of molecules at surfaces

To a crude approximation, STM imaging offers a sub-molecularly resolved map of the tunnelling current in a plane across a conductive sample, probing point by point the probability of tunnelling between tip and surface while scanning. Therefore it renders it possible to select a given molecule and to gain insight into its electronic local density of states (LDOS) at the surface.[15] This is accomplished by sensing the density of filled or unfilled electronic states near the Fermi surface, within an energy range defined by the bias voltage at low voltage.[16] This enables discrimination between different chemical functionalities adsorbed at surfaces.[8,17–20] Even though much attention has been paid to the implementation of theoretical methodologies to supplement experimental results,[20–25] more than 20 years after the invention of STM discrimination between the electronic and topographic structures of surfaces is still a great challenge.

The contrast in STM imaging is determined by the chemical nature of the adsorbate. However, the location of molecules in the plane X–Y with respect to the lattice of the crystalline substrate,[8] and the position of the molecule along the Z axis, *i.e.* molecule–substrate distance,[26] can also generate different overlaps of the frontier orbitals of the molecule with the Fermi level of the substrate. This leads to a different contrast, as the STM provides a picture of the electronic properties of the complex hybrid system which conveys substrate and ad-molecule. Accurate studies revealed that interaction with the conductive substrate induces a strong perturbation of the electronic structure of a synthetic polycyclic aromatic hydrocarbon adsorbed on a highly oriented pyrolitic graphite (HOPG) substrate in the first epitaxial monolayer. In a second epitaxial layer, where the same ad-molecule is 0.335 nm distant from the surface, the molecules are electronically unperturbed (Fig. 1).[27] Previously, a mapping in real-space of the conformation of individual functionalized porphyrin molecules was afforded by STM. It revealed predominantly rotations around the bonds between the porphyrin cores and the to four pendant *tert*-butyl groups, which differ on different metal substrates (Fig. 2).[28] Very recently Ho and coworkers were able to construct a reproducible metal–molecule–metal junction using UHV-STM. In this way electron transport through the single-molecule junction was studied, being determined by the local electronic structure of the nanoscale region that includes the molecule and a number of metal atoms in proximity to the molecule–metal bridge, elucidating the nature of the junction.[29] These results are of great importance for tailoring contacts,[30,31] in view of the future fabrication of nanoscale electronic devices.

A practical approach to visualize self-assembled monolayers and sometimes even multilayers of (macro)molecules adsorbed on a conductive surface is the STM at the solid–liquid interface. In this type of measurement the STM tip is immersed in an almost saturated organic solution in a poorly polar solvent.[8,19,32–36] Interfacial interactions govern the self-assembly at surfaces, that is in competition with solvation in the 3D

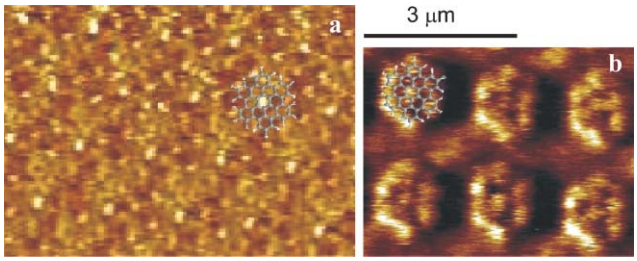

Fig. 1 STM constant height images of self-assembled architectures of hexa-*peri*-hexabenzocoronene (HBC) at the highly oriented pyrolitic graphite–solution interface. (a) Hexagonally packed first layer adjacent to the substrate. The structure possesses a unit cell $a = (1.37 \pm 0.04)$ nm and $\alpha = (60 \pm 1)^\circ$, leading to an area $A = (1.63 \pm 0.05)$ nm^2. The observed features do not reflect the frontier orbital of the neat HBC. (b) Second layer adjacent to the substrate. The unit cell dimensions are $a = (3.7 \pm 0.3)$ nm, $b = (3.6 \pm 0.3)$ nm, $\alpha = (86 \pm 5)^\circ$, and $A = (3.3 \pm 0.3)$ nm^2. The contrasts reflect accurately the nodal planes of the frontier orbitals of the neat HBC. Tunnelling condition of the STM image: (a) $U_t = 351$ mV, average $I_t = 436$ pA. (b) $U_t = 1250$ mV, average $I_t = 125$ pA. Adapted with permission of the American Chemical Society (ref. 27).

supernantant solutions. Exploiting this method ordered monolayers can be easily formed and studied with a sub-molecular resolution. This makes it possible to gain insight into different types of physico-chemical properties that span from the thermodynamics of physisorption at the solid–liquid interface, which is driven by an interplay between the enthalpy gain and the loss in entropy upon adsorption,[37] to the 2D behaviour of chiral molecules at surfaces.[38]

High resolution STM imaging of organic based materials permits remarkable chemical discrimination in organic monolayers and the singling out of physico-chemical properties of a given molecule in an ordered architecture. The possibility to detect smaller and smaller tunnelling currents, together with the ability of supramolecular chemistry to self-assemble more and more complex arrangements, characterised by low

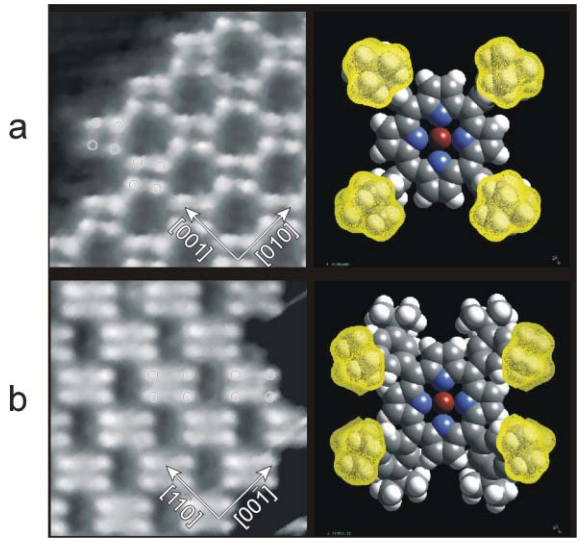

Fig. 2 Conformational identification of Cu-tetra[3,5 di-*tert*-butylphenyl]porphyrin (Cu-TBPP). The four-lobed quadrilateral forms are visible. The lobes appear independently of the variable chemical bonding with the substrates and can be identified as the uppermost *tert*-butyl groups of each of the four large (~1 nm) di-*tert*-butylphenyl units. In the model on the left the four bond angles of the phenyl–porphyrin bonds of each molecule have been determined such that the conformation of the model corresponds to STM data. The uppermost *tert*-butyl groups are shown in yellow to emphasise the molecular subunits visible in the STM data. (a) Cu(100), square symmetry. (b) Ag (110) rectangular symmetry. Scan length = 10 nm. Reprinted by permission from *Nature* (ref. 28) copyright 1997 Macmillian Publishers Ltd. (courtesy of Dr T. Jung).

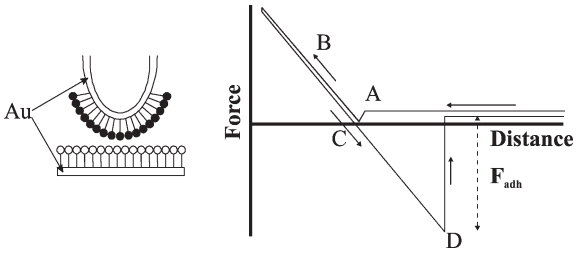

Fig. 3 Schematic representation of a typical Chemical Force Microscopy experiment. The tip, coated with a Au layer, is derivatised with alkanethiols bearing a given functional group in the ω-position (filled circle). The sample surface is coated with a self-assembled monolayer exposing a different functionality (empty circle). By approaching the tip to the surface a force–distance curve can be traced. At position A the tip is attracted to the surface. On decreasing the tip–sample distance a repulsive regime (B,C) is reached. Pulling the tip away from the surface a minimum (D) in the force–distance curve occurs characterised by a maximisation of the tip–surface adhesion due to capillary forces. Continuing the retraction the tip breaks free of surface attraction.

molecular dynamics, will permit insight into nanostructured (bio)organic materials with a high degree of complexity.

Chemical Force Microscopy probing intermolecular interactions

During raster scanning for imaging, SFM measures the force interactions between the tip and the sample surface. Therefore the SFM is basically a force sensor. Besides imaging, the probe of an SFM can also be used to single out directly the forces that hold together two components of a multi-molecular structure. Chemical Force Microscopy (CFM, Fig. 3) combines (i) the force sensitivity of the SFM (down to the sub-nN or even pN scale), (ii) the spatial resolution of SFM (sub-nanometer) and (iii) chemical discrimination. It exploits specifically derivatised SFM tips, prepared covalently linking a self-assembled monolayer (SAM) terminating in a distinct functional group to the tip surface. While the piezo motion of the SPM is frozen in the *XY* directions, the functionalised tip is brought near to the sample surface *via* movement along the *Z* axis. In this way intermolecular interactions between functional groups exposed on the tip and the sample surface can be investigated on the nanometer scale collecting force–distance curves.[39–57] Lieber and co-workers probed the interactions between CO_2H–CO_2H, CO_2H–CH_3 and CH_3–CH_3, revealing the formation of H-bonds between two CO_2H units, weaker forces of van der Waals type between two CH_3 groups, and even weaker interactions between the dissimilar CO_2H and CH_3 moieties.[39,40] The CFM measurements are extremely dependent on the experimental conditions, such as tip and sample composition as well as the surrounding medium.

Capillary forces are caused by the condensation of water vapour in the zone where the tip contacts the sample surface. Given their magnitude of a few nN, they can easily screen weaker interactions such as van der Waals forces or hydrogen bonds. Due to this, measurements need to be performed in either a vacuum, a dry gas atmosphere or a fluid. Conducting the experiments in liquid media, solvent chemical effects on the interaction between organic group assemblies can be analysed. Under these conditions the interaction between two CO_2H groups has been studied in water, 1-propanol and hexane by sampling the approach part of the force curve. While the first case revealed long-range repulsions, due to the presence of electrostatic interactions between the CO_2^- units, in the latter case short-range attractions caused by the formation of H-bonds have been observed.[41] The exploration of pull-out force curves on the interactions between CH_3–CH_3 and CO_2H–CO_2H has shown that solvent exclusion can directly affect the adhesive forces between the tip and the surface, an effect which is more pronounced in water and on the CH_3–CH_3 pair.[42]

The CFM study, which has also been extended to other moieties including NH_2 and OH, has also been performed as a function of the ionic strength and of the pH. This permitted the generation of adhesion force titration curves on the nanoscale, and thus determination of the pK_a which resulted in similar values to those obtained by conventional contact angle wetting studies of the same surfaces.[43] This method for determining the pK_a has also proved to be viable for probing, at different pH, the interaction between two dissimilar groups, namely NH_2 and OH.[44]

Chemical reactions such as the hydrolysis of ester groups in self-assembled monolayers (SAMs) have been monitored with the so-called inverted CFM. In the latter, the chemical reaction taking place at the surface of the tip coated with reactants, is probed *in-situ* by force–distance measurements on a scale of less than 100 molecules. The pull-off forces of different reactive SAMs provided evidence of the occurrence of reaction.[45]

Recent success in chemical mapping of the surface functionality of oxidized polymer films with sub-50 nm resolution using CFM[58] points to the need to move to more complex, chemically heterogeneous systems, such as polymers, mixed monolayers, or supramolecular architectures. In this concern, the cation complexation force of 18-crown-6 has been measured in ethanol by means of CFM using probe tips and mica substrates modified chemically with 18-crown-6 and ammonium ion, respectively. The specific complexation force was suppressed by free potassium ion in the measurement solution, indicating a blocking effect based on the competitive complexation of the 18-crown-6 moiety between the free ion and the ammonium ion bound to the substrate. The single complexation force of 18-crown-6 with ammonium ion in ethanol was evaluated to be about 60 pN.[59] Also in line with increasing complexity, Frisbie and co-workers have studied the chemical binding force of discrete electron donor–acceptor complexes under $CHCl_3$. CFM studies on the interaction between *N*,*N*,*N*′,*N*′-tetramethylphenylenediamine (TMPD) and the electron acceptor 7,7,8,8-tetracyanoquinodimethane (TCNQ) revealed a force–distance curve with a (70 ± 15) pN periodicity, assigned to the rupture of individual of TMPD–TCNQ donor–acceptor (charge-transfer) complexes.[55] This opens perspectives for the investigation of complex binding phenomena which can depend on external stimuli such as light.

CFM is also a chiral sensor. McKendry and co-workers have shown that one can discriminate between enantiomers of mandelic acid at the near-molecular level. Two types of (*R*)- and (*S*)- derivatives of mandelic acid were bound to gold surfaces. The differentiation of (*R*)- and (*S*)-mandelic acid was achieved exploiting chiral selectors such as the (*R*)- or (*S*)-phenylglycine derivative that were bound to the tip. The different interactions between the enantiomers gave rise to different adhesion forces, which were used to achieve the discrimination. Importantly, to minimise variations in data determined by the use of different tips, measurements were performed employing a single tip on each of the different chiral surfaces investigated. These results were properly confirmed by collecting sixty measurements of adhesion forces on each surface as well as by checking the integrity of the tip by repeating the measurement of the first surface at the end of the sequence.[60]

Most of the CFM results can be well described by the Johnson–Kendall–Roberts (JKR) theory of adhesion mechanics.[39,40,55,57] A hybrid molecular simulation approach that combines a dynamic model for the CFM tip-cantilever system and a molecular dynamics (MD) relaxation technique for SAMs on Au(111) at room temperature has been applied to investigate dynamic adhesion and friction between a CFM tip and a substrate, both modified by self-assembled monolayers (SAMs) with hydrophobic CH_3 or hydrophilic OH terminal groups. This permitted for the first time the simulation of force–distance (or adhesion) curves and friction loops (or

friction coefficients) in the CFM on the experimental time scale. In good agreement with experimental data, the simulation showed that the adhesion force and friction coefficient for the OH–OH contact pair are much larger than those for the CH_3–CH_3 pair due to the formation of hydrogen bonds.[61] More recently, atomistic molecular dynamics simulations have been successfully employed to gain deeper understanding into the experimental results obtained with CFM on the interaction between a tip coated with an alkanethiolate self-assembled monolayer interacting with a smooth planar solid-wall.[62]

Therefore, adhesion force measurements between different surfaces under different media can provide notable insights that are crucial to understand and control intermolecular interactions. This approach is very helpful to determine qualitatively the magnitude of the interaction between different units, albeit it lacks a quantitative determination of the forces since one can hardly estimate the number of functional groups that are probed in each measurement! Thus we can not offer an exact quantification of the strength of the broken bond.

Exploiting a derivatised tip one can also image the surface with SFM achieving a chemical sensitivity, due to the different intermolecular interactions between the tip and the chemical functionality exposed on the sample surface. This sensitivity was evidenced by visualising nanopatterned surfaces.[43,56,57] Unfortunately this approach suffers from degradation of the tip, which is due to the presence of frictional forces between the tip and the surface during raster scanning.

The SFM set-up cantilever can be used to monitor biochemical reactions such as the specific transduction, *via* surface stress changes, of DNA hybridisation and receptor–ligand binding into a direct nanomechanical response of microfabricated cantilevers. Arrays of cantilevers were derivatised with diverse biomolecules. The differential deflection of the cantilevers was found to offer a true molecular recognition signal despite large non-specific responses of individual cantilevers. Hybridisation of complementary oligonucleotides revealed that a single base mismatch between two 12-mer oligonucleotides can be detected.[63] Using this method nanomolar concentrations of different unlabeled DNA sequences can be detected within minutes and it can discriminate overhangs through differential measurements. The nanomechanical response originates predominantly from steric hindrance effects and it is sensitive to the concentration of oligonucleotides in solution; thus one can estimate how much of a given biomolecule is present and active. The specificity of the measurements is determined by the thermodynamics of the ligand–receptor binding interaction on the cantilever, which enables the measurement of thermodynamic equilibrium constants.[64]

In summary CFM studies grant insight into the thermodynamics of supramolecular interactions and allow chemical reactions to be monitored. Combining this approach with external stimuli, complex interactions and related phenomena occurring in nature can be explored.

Mechanical properties of macromolecules

SFM imaging to explore different physico-chemical properties

SPM imaging itself already permits the characterisation of a large number of physico-chemical properties of isolated molecules as well as of complex multimolecular arrangements. Besides being tools for the direct quantification of the molecular weight distribution of polymers,[65,66] SFM makes it possible to study conformational and mechanical properties of single (macro)molecules[67,68] or of supramolecular architectures.[69,70] Kinetic experiments on the adsorption of dsDNAs revealed that the transport of these molecules from the solution drop onto the surface is governed solely by diffusion, and that the molecules are irreversibly adsorbed onto the substrate. A statistical polymer chain analysis was applied to dsDNA molecules to determine the deposition conditions that lead to equilibrium and those that result in trapped configurations. Using the appropriate conditions, DNA molecules deposited onto freshly cleaved mica can be equilibrated in quasi 2D on a surface as in an ideal 2D solution. A persistence length (l_p) of 53 nm was determined from those molecules. This value agrees with the ones obtained in solution using more indirect scattering methods.[71] Macromolecules that do not equilibrate on the surface adopt conformations similar to those expected for a simple projection onto the surface plane, suggesting a process of kinetic trapping. Later, synthetic polymers of isocyanodipeptides have also been investigated using a similar approach, based on a Tapping Mode SFM[6,7,72] study of the conformation of isolated macromolecules equilibrated at a surface. For this macromolecular system the l_p was determined as (76 ± 6) nm[73] which is more than one order of magnitude larger than the l_p determined in solutions for simpler poly(isocyanides), namely poly(α-phenylethylisocyanide).[74] This indicates that the hydrogen bonded networks existing in the side-chains of the polymers stabilize the overall polymer structure in line with previous physico-chemical studies.[75] Among single chain synthetic polymers the stiffness of the poly(isocyanodipeptides) is indeed very high, having an l_p that is even 50% larger than that of dsDNA.[71]

By studying the dynamics of the oscillating tip-cantilever systems while imaging complex films such as triblock copolymers with tapping mode SFM one can gain insight into the local mechanical properties of the multicomponent architecture and discriminate them from the topographical contribution to the overall image contrast,[76] as well as to cast light onto the viscosity of the film on the nanometer scale.[77,78]

The Pulsed Force Mode (PFM) extends the capabilities of SFM. In addition to the sample topography, the PFM offers access to material properties such as local stiffness and adhesion on a micro- and nanometer scale, while the lateral forces are virtually eliminated. Therefore, high resolution mapping of delicate samples in air and fluids can be attained.[79] PFM can be used to study both mono- and multicomponent ones. A series of investigations on phenylene-based dendrimers[80] allowed insight to be gained into the adhesion on mica of different dendrimers with increasing generation either with[81] or without[69]carboxyl groups in the outer rim. In a different set of experiments, adhesive forces and topography were mapped simultaneously on single poly(sodium 4-styrenesulfonate) (PSS) polymers supported on a rough surface. Force–distance curves showed the differences in adhesive forces of the tip/sample and the tip/surface couples, so that sample materials can be distinguished in terms of surface adhesive properties.[82] A wealth of information can be gained exploiting PFM on multicomponent films. A good example of this can be found in ref. 83 where PFM was used to study the morphology of three segmented polyurethane elastomers. High-contrast images provided evidence of the phase-separated structures on a scale of several tens of nanometers to a few hundred nanometers. The adhesion-dependent pull-off force signal was found to be far more sensitive to local variations in mechanical properties than the stiffness-dependent indentation force signal.[83]

In conclusion, imaging itself offers access to a huge amount of information on the nanomechanics of molecule based nanostructures. The combination of imaging with SPM manipulation (see below) will open more intriguing perspectives in the fields of polymers and materials science.

Force Spectroscopy (FS)

Making use of an approach similar to CFM, either the forces that hold together two components of a complex macromolecular architecture or the mechanical properties of single polymer chains can be probed. This can be done by tethering

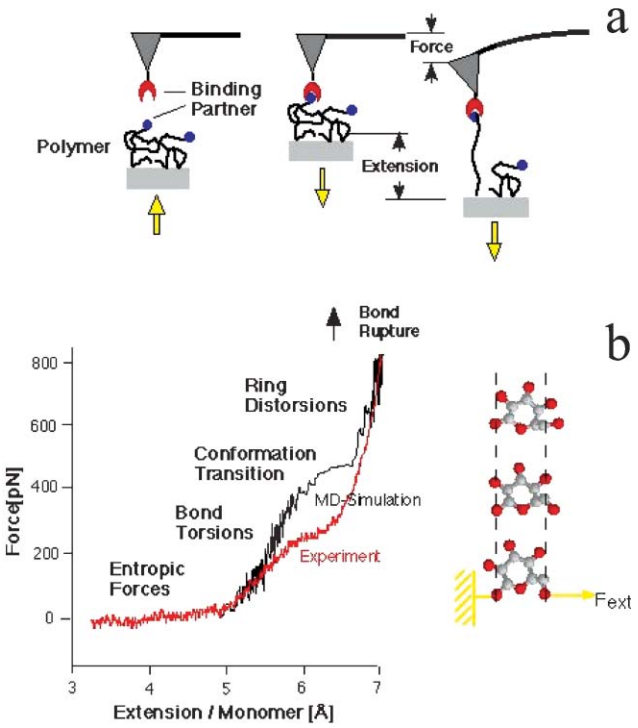

Fig. 4 (a) Schematic representation of a Force Spectroscopy experiment. The functionality attached to the SFM tip selectively binds a pendant group from the macromolecule adsorbed on a surface. Pulling the tip away from the surface the macromolecule is stretched. (b) At increasing extension, different types of conformational transitions are prompted.

the (macro)molecular object both to the SFM tip and to the surface. Sampling force–distance curves, thereby manipulating molecular objects along the *Z*-axis with the SFM tip, one can induce a rupture of the weaker bond in the system or induce a mechano-chemical transition, producing a restoring force that causes the bending of the cantilever (Fig. 4). This methodology, known as Force Spectroscopy (FS), in the best cases permits spatial manipulations of less than a nanometer and can detect forces in the piconewton (pN) regime.[84] The development of smaller, softer and more drift-stable cantilevers will allow these limitations to be partially overcome.[85] Due to the same reasons related to capillary forces explained for CFM, FS measurements must be conducted in a liquid medium. Under this latter environment one can also study biological processes, such as binding and unbinding, as well as nanomechanical properties of isolated biomolecules.

A milestone in FS investigations was the direct measurement of the rupture of bonds formed in a ligand–receptor complex, namely between streptavidin and biotin.[86,87] By blocking many biotin or iminobiotin sites on the surface and fully functionalising the tip with avidin units, it was possible to detach a few bonds at a time and determine the rupture occurring at (160 ± 20) pN between avidin and biotin and at (85 ± 15) pN between avidin and iminobiotin.[86] In these experiments the molecules under investigation did not need to be attached covalently to the tip and sample, but rather physisorption was used successfully. This was done by picking up a different part of the individual chain with the SFM tip applying a contact force of several nN over a period of seconds. The obtained unspecific attachment was stable under forces up to a nN.[88] Using this experimental set-up Rief and collaborators have successfully unzipped the double strand of DNA, singling out forces necessary to break A–T bonds as 9 pN, while 20 pN was required to split C from G.[88]

Making use of this knowledge, very recently a short DNA duplex with a given sequence, which thus possesses the

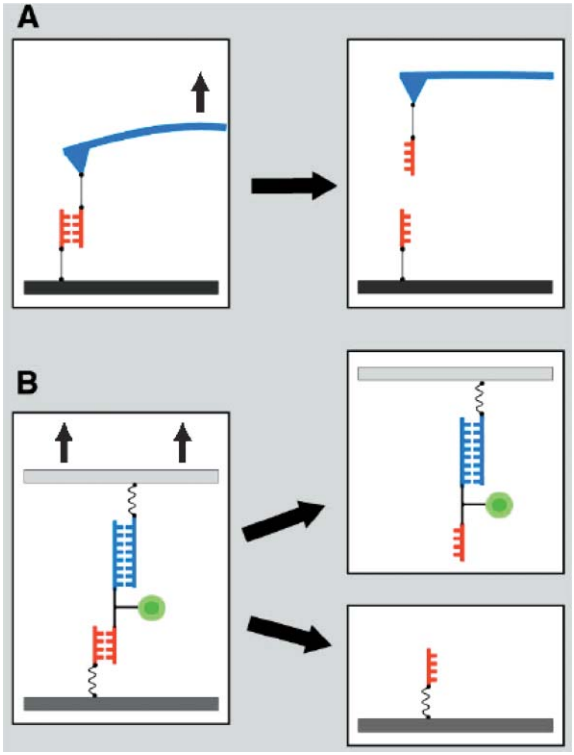

Fig. 5 (A) Conventional FS experiment in which the rupture force required to break a molecular bond, such as a DNA duplex (red), is measured with a cantilever spring (blue). (B) The differential force test, in which the rupture force of a sample bond (red) is measured by comparing it with a known reference bond (blue), which serves as a molecular force standard. Upon loading the chain of polymer spacers, sample bond, and reference bond, the weaker bond has a higher probability of rupturing than the stronger one. Consequently, most of the probed fluorescence labels (green) end up with the stronger bond after separating the two surfaces. Reprinted with permission from ref. 89. Copyright 2003 AAAS.

previously defined bond strengths, has been employed as a molecular force standard in a FS experiment that aimed at the quantification of intermolecular interactions (Fig. 5). During separation of the two surfaces a complex nanostructure which conveys a sample and the reference was stretched, until the weaker among the two bonds got broken.[89] The discrimination between different binding modes and the concept of mechanical stringency offers striking advantages when applied to the field of protein arrays. In fact employing the threshold force defined by the short DNA sequence one can discriminate between specific and non-specific binding in a variety of antibody–antigen interactions.[89]

The intrinsic elasticity of polysaccharides has also been explored at the single molecule level making use of FS. Dextran and amylose exhibited similar mechanical properties under extension. At low force the force–curve revealed a range governed by an entropic contribution. At higher forces an intramolecular structural transition took place, increasing its effective length. In contrast, for cellulose although its chemical structure is very similar to that of amylose, it did not show any conformational transition.[90]

When the bond to be broken has a strength in the nN range or even higher values, it turned out to be necessary to tether covalently the molecule to the two surfaces. This strong anchoring has been employed by Grandbois and co-workers on single polysaccharide strands; these chains have been stretched until breakage of covalent bonds. While a bond between silicon–carbon exhibited a strength of (2.0 ± 0.3) nN, the one between sulfur–gold revealed values of (1.4 ± 0.3) nN. Bond rupture probability calculations, based on density functional theory, nicely supported the experimental results.[91]

SFM imaging has been used in conjunction with FS to gain more information during a pull-out experiment. The imaging made it possible to monitor an individual molecule before and after its manipulation. In this way it was possible to determine the intermolecular forces between single proteins on a bacterial surface layer and to shine light onto the unfolding pathway during the pulling out process.[92]

Interestingly for polymer scientists, single polymer chains can be attached to the tip and substrate and stretched. In the relaxed state the polymer tends to adopt a coiled conformation due to the maximisation of the entropy of its segments. The extension of the macromolecule generates an opposing force because of the entropy decrease. Small extensions require a limited force; however, the resistance to the extension increases as the polymer approaches its stretched conformation. The worm-like chain model (WLC) describes well the mechanical behaviour of the polymer under this type of stress.[93,94]

Most importantly, FS does not suffer from the averaging of a heterogeneous pool of data, but rather offers insight into the distribution of the observables. This makes it possible to single out sub-states which are commonly averaged out in microscopic investigations. For example it has been shown, in the first instance, on the muscle protein titin,[95] and later on other multi domain proteins, that the modules can be unfolded one by one. The so-obtained force curve is characterised by a saw-tooth pattern with a number of peaks corresponding to the domains that have been unravelled (Fig. 6).[84,96] The mechanical behaviour therefore deviates from a pure entropic contribution in the polymer extension.

The possibility of tuning the constant pulling rate and the temperature of the system allows attainment of a thermodynamic quasi-equilibrium condition and to discern between the enthalpy and entropy contribution, respectively.[97,98] Alternatively, making use of the Jarzynski equality relating the irreversible work to the equilibrium free energy difference ΔG, one can obtain equilibrium thermodynamic parameters from processes carried out arbitrarily far from the equilibrium.[99]

By and large, FS offers the chance to exert external forces to modify the extent and even alter the fate of reactions with the intent to extrapolate rules that govern the interconversion of mechanical and chemical energy in these processes.[100]

FS is also an ideal set-up to probe mechano-chemical processes induced by external stimuli. The optical excitation on an azo-benzene based architecture, inducing a switching between the *cis* and *trans* configuration, was detected on isolated molecules. This represented the first example of opto-mechanical energy conversion at the single molecule level.[101]

FS measurements are all about grabbing the cat by the tail.[100] Exploiting this crude game for manipulating single molecules, material scientists will be able to explore the nature of (bio)molecular machines one at time, and infer from their behaviour those properties common to the population and those corresponding to specific sub-states.

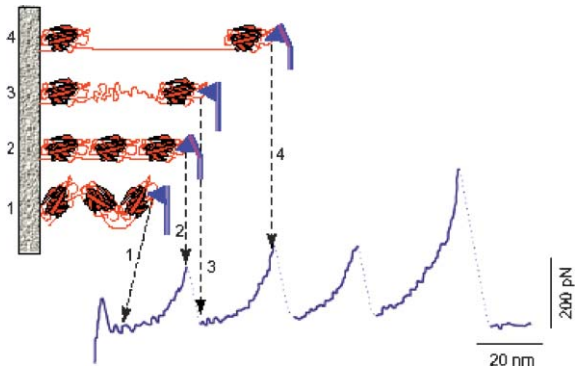

Fig. 6 The entropic elasticity of a multimodular protein and its domain unfolding. The saw-tooth pattern of peaks, observed when force is applied to extend the protein, corresponds to sequential unravelling of individual domains of a modular protein. As the distance between substrate and cantilever increases (from state 1 to state 2) the protein elongates, generating a restoring force that bends the cantilever. When a domain unfolds (state 3) the free length of the protein increases, returning the force on the cantilever to near zero. Further extension again results in force on the cantilever (state 4). The last peak represents the final extension of the unfolded protein prior to detachment from the AFM tip. Printed with permission of Elsevier from ref. 84.

Nanomanipulation

New avenues of exploration are accessible by exploiting nano-manipulators running on SPM set-ups. These tools are based on a fine tuning of the position of the SPM tip relative to the sample surface. This permits control of the interaction between tip and surface and to exploit the sharp tip in an invasive way triggering a variation of the morphology or of the structure of a thin film with a molecular scale precision. In this way SPM heralds its ability both to fabricate and to monitor high-resolution, miniaturised molecular arrays. These types of manipulations have been performed typically at very low temperature, a few Kelvin, and in very controlled environments, ultra-high vacuum (UHV).

Under these conditions the dynamics of the single ad-molecules is pretty small, thus one can approach them with a good precision with the SPM tip after having imaged them. An impressive result was reported by Eigler and co-workers employing the STM to position 48 Fe atoms into a circular ring in order to "corral" some surface state electrons and force them into "quantum" states of the circular structure (Fig. 7). This allowed visualisation and study of the quantum mechanical properties of electrons which are confined to dimensions as small as possible for future electronic devices.[102]

In 1996 Gimzewski and Joachim demonstrated that one can simplify the experimental conditions and manipulate single porphyrins[103] and fullerenes[104] at room temperature in UHV. In this latter experiment, a molecular scale prototype of an abacus was fabricated, where single fullerenes were translated along the Cu(111) monoatomic steps by using the STM tip as manipulator.

Sub-monolayer quantities of π-conjugated molecular species have been deposited in UHV on metallic surfaces and the tip of a STM has been employed to manipulate single molecules *in-situ*, shining light on the internal mechanics of the molecules

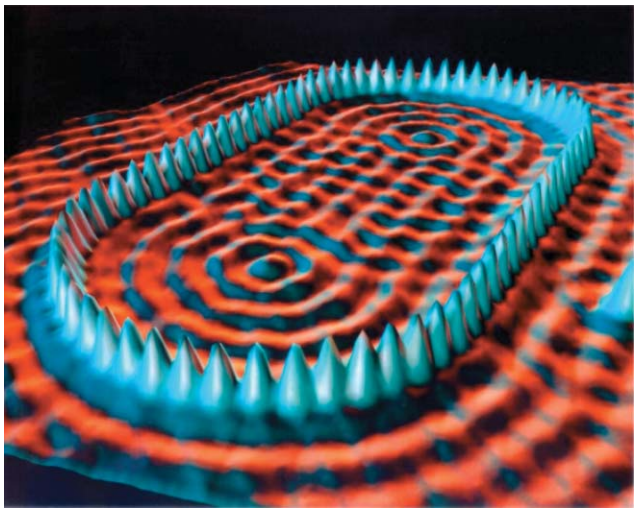

Fig. 7 Single Fe atoms adsorbed on a Cu(111) surface forming a "quantum corral" at 4 K. The image shows the contour of the local density of electron states. The corral is about 14.3 nm in diameter. The ripples in the ring of atoms are the density distribution of a particular set of quantum states of the corral. Reprinted with permission of ref. 102. Copyright 1993 AAAS.

and inducing conformational molecular switches.[103,105–107] This represents a step forward towards the fabrication of molecular tunnel-wired nanorobots.[108] Moreover the manipulation of individual molecules on a conductive substrate allows their placement at desired positions on the surface. This method was applied to move polycyclic aromatic hydrocarbons (PAHs) to a double atomic step of the Cu(100) surface that could then act as a well-defined electrode. The tip of the STM was employed as a counter-electrode, and in this way the conductivity of the single molecules along the main molecular axis was probed.[109]

Making use of a non-contact SFM and STM operating in UHV, the switching energy of a single molecule switch based on the rotation of a di-butyl-phenyl leg in a Cu-tetra-3,5 di-*tert*-butyl-phenyl porphyrin was determined. The mechanics and intramolecular conformation of the switched leg was controlled by the tip apex of the non-contact SFM. The comparison between experimental and calculated force curves revealed that the rotation of the leg requires an energy less than 100×10^{-21} J, which is four orders of magnitude lower than state-of-the-art transistors.[110]

Later the manipulation also became viable at room pressure under mild environmental conditions. Individual tobacco mosaic viruses were visualized and manipulated at the graphite–air interface, and data revealed a competition between sample–substrate lateral friction and the flexural rigidity of the manipulated object.[111] Circular DNA was manipulated at the solid–liquid interface. After its imaging the DNA was cut with the SFM tip by applying a local pressure. Visualisation after the manipulation showed that the linearised molecule started searching amongst conformations with a higher end-to-end distance than its initial zero value.[112]

The tip of a SFM, operating in contact mode, has been employed to induce a mechanical perturbation whose effect is localised at the contact area of the tip (Fig. 8). The experiments

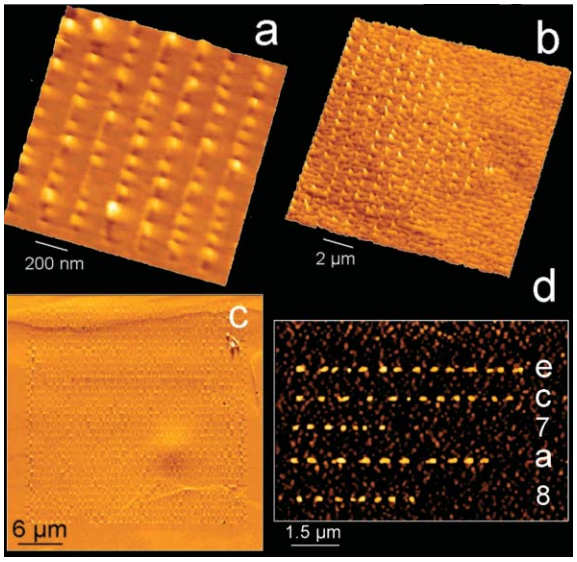

Fig. 8 (a) Array of dots of an amide-based rotaxane produced by individual line scans of the SFM tip on a 5 nm-thick film adsorbed on HOPG. (b) For a given thickness (here 20 nm), the number of dots is linearly proportional to the scan length. The number of dots can be determined with a 2% accuracy. Film thickness controls the characteristic size. Changing the film thickness in the range between 3 and 35 nm, the interdot distance increases from 100 to 500 nm, the dot full-width-half-maximum from 40 to 250 nm, and the dot height from 1 to 20 nm, with a dispersion of 10 to 20%. (c) Pattern made of 31 lines with 45 dots each on a 30×30 μm^2 area on a thicker film. (d) Proof-of concept for information storage. The sequence "e c 7 a 8" in the hexadecimal base corresponds to the number 968616. Reprinted with permission from ref. 113. Copyright 2003 AAAS (courtesy of Drs M. Cavallini and F. Biscarini).

performed on thin films of benzylic-amide-based rotaxanes revealed that a local, collective reorganisation of the material into spatially correlated nano-dots occurs when the tip is scanned along a line with a load force just above a 2 nN threshold. These manipulations were performed on the (sub)micrometer scale, thus there was no direct control of conformational transitions at the level of single molecules. The authors believe that the fact that a collective writing of an array of nanostructures occurs, is possibly related to the interconversion of rotaxanes in the solid state and to formation and ripening of crystalline nuclei.[113]

Very recently Rabe and Schlüter were able to manipulate single rod-like dendronised polymers with the SFM tip,[114] and connect two strands covalently performing a photochemical reaction at surfaces (Fig. 9).[115] The "move-connect-prove" approach was used to attest the formation of the new single polymer chains starting from the two smaller units.[115] This represented an important step forward towards the nano-construction and generation of nano-archichitectures at will.

Differently from SFM, the STM permits achievement of higher spatial resolution in the imaging, and the manipulation can be addressed down to the single molecule scale. Unfortunately manipulations with STM cannot be performed on self-assembled monolayers at the solid–liquid interface since under these conditions the interfacial interactions are very strong and the dynamics of the molecules are extremely high; once the tip is retracted from the "manipulating mode", the monolayer having the initial supramolecular arrangement is formed again, due to the strong interfacial interactions governing the self-assembly. A solution to this problem was recently introduced.[116] Starting from STM exploration at the solution–solid interface, evaporation of the solvent led to the formation of a gel which was stable on the substrate surface for several days. As an example, crown ether-functionalised phthalocyanines were investigated under these conditions [Fig. 10(d)]. Sub-molecularly resolved STM imaging exhibited the co-existence of three different arrangements over an area of some hundreds of square nanometres. Two (1 and 2) highly ordered 'face-on' hexagonal phases, and another one (3) arranged 'edge-on', forming lamellae consisting of π–π stacked phthalocyanines. Because of the durability of this gel–graphite interface, it became possible to execute STM measurements continuously for a few days with the tip immersed in the gel. In addition, the slow dynamics of the single molecules at this interface made it possible not only to follow the coarsening of a single molecule over a timescale of several hours, but also to readily manipulate the molecular adsorbate with precision on the molecular scale. In this set of experiments, after having 'read' the surface [Figs. 10(a) and (d)], the tip of the STM was employed in an invasive mode to 'write' information on the molecular scale [Fig. 10(b)]. This could be accomplished by reducing the tunnelling gap impedance, thus inducing a mechanochemical switch from the 'face-on' to 'edge-on' packing. Going back to non-invasive measurement conditions, the surface was 'read' again and the switching which took place in area 4 was monitored [Figs. 10(c) and (e)].[116]

All in all, nanomanipulation offers perspectives for future explorations on the nanomechanics of complex arrangements as well as for the nanoconstruction of surfaces, being of paramount importance in the frame of increasing the density of data storage.

Nanolithography with SPM

To date, different methodologies have been introduced for nanopatterning surfaces exploiting the SPM tip as an active pen. Among them, Dip-Pen Nanolithography (DPN) turned out to be a pretty simple and viable approach: the SFM tip is employed to deliver molecules to a surface *via* a solvent meniscus, which naturally forms in the ambient atmosphere

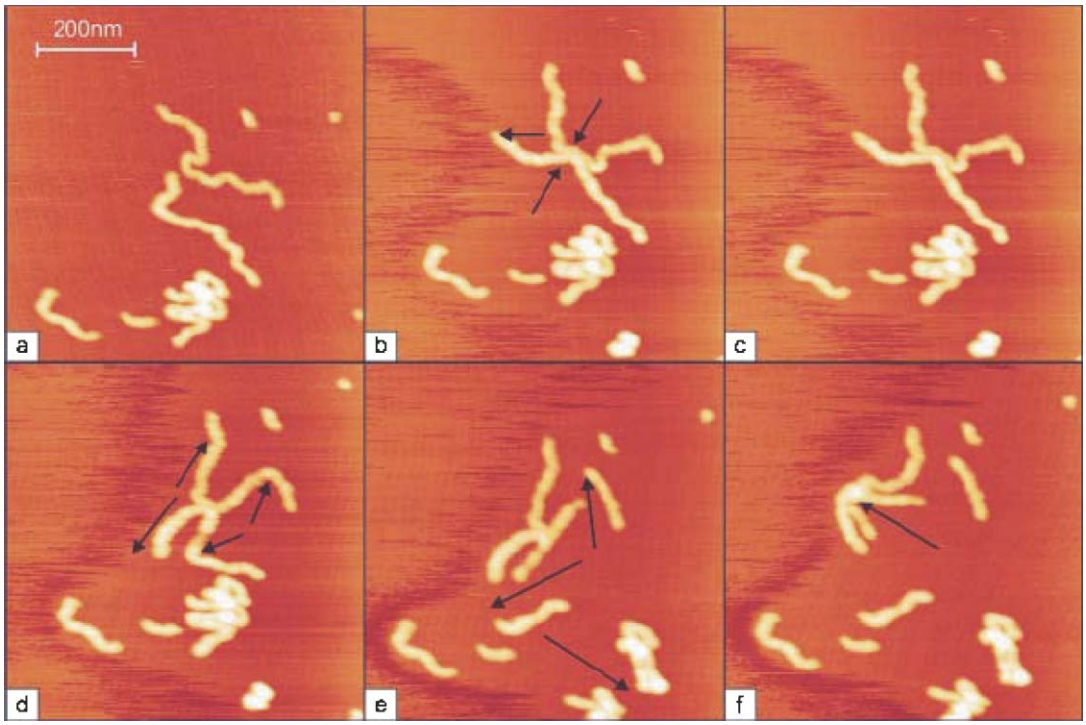

Fig. 9 Tapping-mode SFM images of two individual dendronised polymers, moved towards each other ("move"; a–b), irradiated by UV light ("connect"; b–c), and challenged mechanically ("prove"; d,e,f). The arrows indicate the movement of the SFM tip during manipulation. Reprinted with permission from *Angew. Chem., Int. Ed.* (ref. 115) copyright 2003 Wiley-VCH.

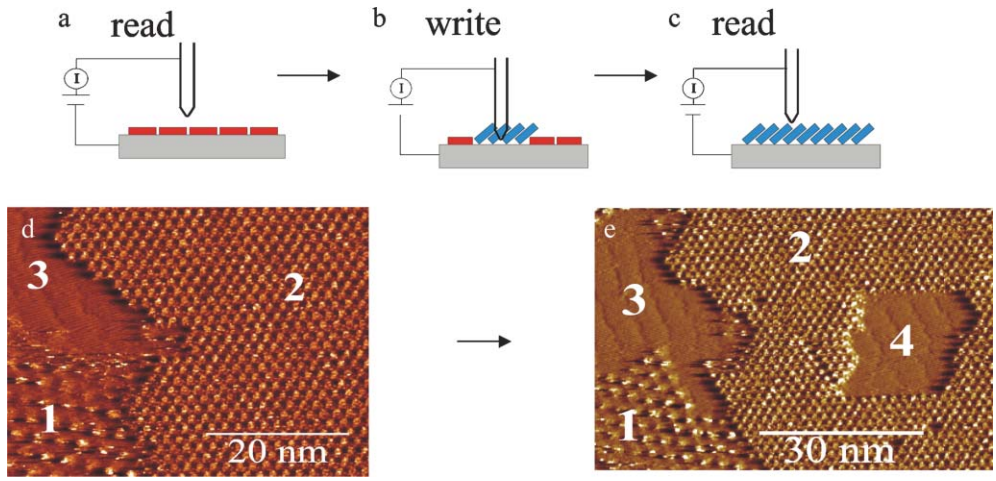

Fig. 10 Scheme showing the STM tip being employed to (a) 'read a surface', (b) 'write a surface', and (c) 'read a surface' again. The STM images were recorded at the gel–HOPG interface: (d) reading the surface before manipulation; (e) reading the surface after manipulation. The area indicated by 4 in (e) has been manipulated by inducing a mechano-chemical switch from the 'face-on' hexagonally packed structure to the 'edge-on' lamellae architecture. Reprinted by permission from IOP Publishing Limited (ref. 117) copyright 2002.

(Fig. 11). This direct-write technique offers high-resolution patterning capabilities for a number of molecular and biomolecular 'inks' on a variety of substrate types such as metals, semiconductors, and monolayer functionalised surfaces thereby tailoring nanostructures composed of organic,[118,119] semiconducting,[120] or metallic materials[120,121] with controlled and well-defined nanometer shape and size.

More precisely, in analogy with a quill pen, the SFM tip is simply coated with a molecular 'ink' and then brought into contact with the surface to be patterned. Water condensing from the immediate environment forms a capillary between the SFM tip and the surface, which in some cases aids transport of the ink molecules onto the substrate. In other cases, a chemical or physical driving force, such as chemisorption of atoms or electrostatic interaction, is used to assist molecular transfer of

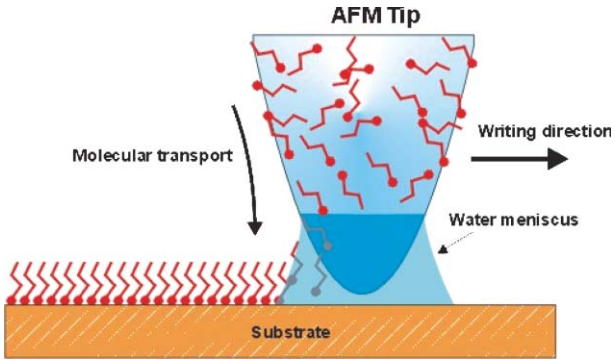

Fig. 11 Cartoon of Dip-Pen Nanolithography (DPN). Reprinted with permission from ref. 118. Copyright 1999 AAAS.

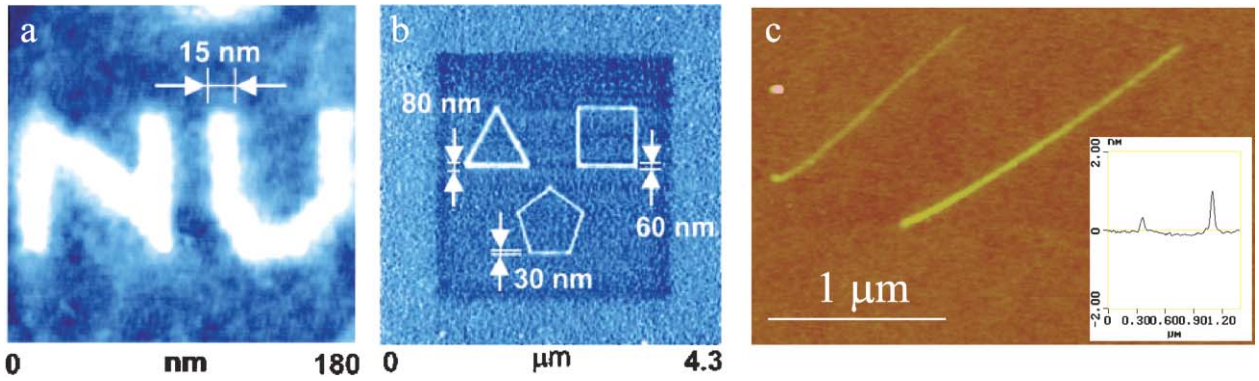

Fig. 12 (a) Nanoscale molecular letters written on an Au(111) surface with 16-mercaptohexadecanoic acid (MHA) molecules by DPN. (b) SAMs in the shape of polygons drawn by DPN with MHA on an amorphous Au surface. A 1-octadecanethiol SAM has been overwritten around the polygons. (c) Two straight poly(3,4-ethylenedioxythiophene) (PEDOT) written by electrochemical dip-pen at 10 (left) and 1 nm s^{-1} (right). The humidity was 28% and the voltage was −12 V. Polymer line width: 50 nm scale bar: 1 μm. Inset: Cross-section of the two lines. Reprinted with permissions: (a,b) from ref. 123 (Copyright 1999 AAAS) and (c) from the American Chemical Society (ref. 127).

the ink from the tip to the surface. Keeping the SFM tip static, spots can generated on the substrate surface, while lines and curves can be produced by moving the probe during ink deposition. The DPN experiments need to be performed in a controlled environment where humidity levels can be tweaked to optimise transport.[122]

The DPN was first introduced in 1999 by Mirkin, demonstrating how this method can be easily applied to fabricate alkanethiol nanostructures onto a gold surface (Fig. 12a).[118] Multicomponent nano-architectures were also designed by DPN using multiple ink (Fig. 12b).[123] Moreover, the use of multiple tips at the same time permits parallel and serial writing capabilities.[124] With DPN protein nanoarrays[125] as well as modified nucleotides[126] have been self-assembled at surfaces, opening new avenues towards the study of fundamental interactions between biological systems such as biomolecular recognition, association, and binding.

Combining the dip-pen with the electrochemical approach,[120] poly-thiophene nanowires on semiconducting or insulating substrates have been designed. Starting from the monomer, polymeric π-conjugated wires were fabricated with a length of several micrometers (Fig. 12c).[127]

Using the same tool poly-histidine-tagged peptides and proteins, and free-base porphyrins coated on SFM probes, were chelated to ionised regions on a metallic nickel surface by applying an electrical potential to the SFM tip in the DPN process.[128] Exploiting an electrochemical approach, Sagiv and co-workers have implemented a facile route to nano-pattern a self-assembled monolayer, supported on a silicon wafer, with some metallic silver nanodots. Starting with a thiol-top-functionalized silane monolayer (TFSM) with silver ions chemisorbed on its outer surface (Ag^{+}–TFSM), metallic silver nanoparticles were generated at selected surface sites by either wet chemical or tip-induced electrochemical reduction of the surface-bound metal ions.[129] This demonstrated that nanolithography is a versatile way to the *in-situ* chemical fabrication of spatially defined metal structures on organic monolayer templates.

Alternatively, different types of nanostructures can be fabricated from a self-assembled monolayer of thiolates on gold by exploiting the tip in an invasive mode. These modes are shown in Fig. 13. In nanoshaving (Fig. 13A) the SFM tip exerts a high shear force during the scan, which causes displacement of the SAM adsorbates. Performing this manipulation at the solid–liquid interface using a solution containing a different alkanethiol, one can induce the occurrence of chemisorption in the newly exposed gold surface as the tip ploughs through the matrix SAM, in the so called nanografting mode (Fig. 13B). In both cases reducing the interaction forces between the tip and the sample surface, one can visualize the nanostructures in a non-invasive fashion.

Making use of STM, nanolithography can also be performed on the nanoscale. After imaging the alkanethiol monolayer in UHV with a low average tunnelling current, by increasing the tunnelling current beyond a certain limit, one can induce the displacement of metal atoms (electron induced diffusion, Fig. 13C) or the desorption of adsorbate molecules (electron induced evaporation, Fig. 13D).[130]

Combining conducting SFM (see below) with nanoshaving, the surface can be visualized and patterned with different molecules by the same tip, and at the same time the electron transfer properties of the surface can be explored and correlated with other properties such as the topography.

Therefore a number of viable approaches are already established for nanoconstruction by manipulating materials with a nanoscale precision exploiting the SPM tip. Even though these methods are difficult to employ on the industrial scale, they will be fundamental in a variety of fields where tailoring

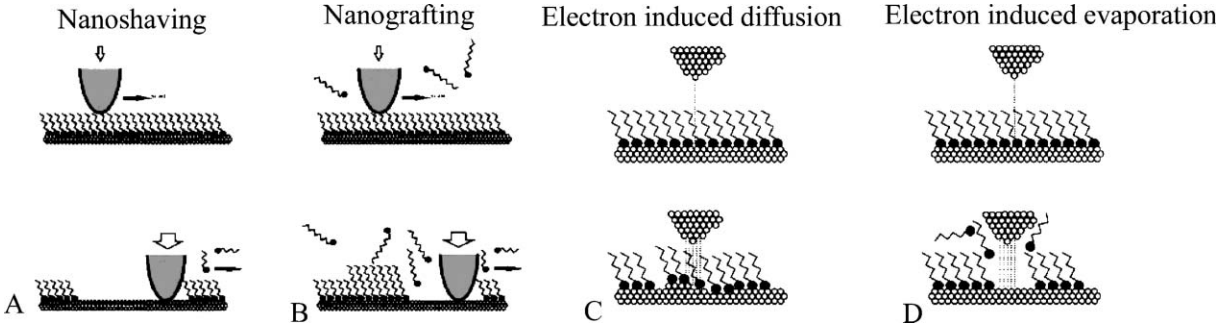

Fig. 13 Cartoons of four manipulation modes exploiting SFM (A and B) and STM (C and D). The imaging and fabrication modes are depicted in the top and bottom rows, respectively. Reprinted with permission of the American Chemical Society (ref. 130).

small objects can offer a step forward towards the generation of smarter materials and functional devices.

Tip activated chemical reactions

The tip of the STM can be exploited to direct chemical reactions with a molecular scale precision.[131] The sharp STM tip can be used to break bonds selectively, to manipulate molecular fragments and to form new bonds. This series of operations was accomplished by performing an Ullmann reaction involving the homocoupling of two iodobenzene molecules to afford biphenyl.[132,133]

Topochemical reactions were also carried out at surfaces by using the STM tip as stimulus. This requires a careful molecular design which offers a well-defined relative orientation of the reactive moieties. In this way intermolecular reactions can take place. A typical example is the topochemical reaction between diacetylenes giving rise to poly-diacetylenes. Besides the previously performed polymerisation at surfaces triggered by light,[134] Aono has shown that the STM tip can be used to "draw" a 1D π-conjugated polymer (poly-diacetylene), applying a pulsed sample bias from a predetermined position in a self-assembled monolayer of diacetylenes at surfaces.[135,136] Very recently, De Schryver and co-workers have demonstrated that by exploiting the same procedure one can successfully write 2D nanostructures on graphite.[137] This method represents a new way for the nanofabrication of electrically active species, which is of great importance in the frame of tailoring nanoelectronic circuits. More generally, the tip induced reaction will make it possible to promote complex reactions in a given location at surfaces and to cast light onto their mechanism.

Electrical properties

The electrical properties of nanostructures can be elucidated by means of different types of SPMs. All of them permit combination of a high resolution structural characterization with electrical measurements, paving the way towards the correlation of nanoscale structure with the transport properties in molecule based materials. They differ in the type of spatial resolution they can achieve and in the type of conductivities that are measured. Being based on the quantum chemical principle of the tunnelling of electrons, STM offers superior spatial resolution in imaging and it allows to wire a smaller amount of molecules per measurement. Differently exploiting the SFM based modes one can obtain a true topographic map of the investigated nanostructure, despite the larger contact area in the electrical measurements.

Scanning Tunnelling Spectroscopy (STS)

Beyond imaging, the STM set-up can supply spectroscopic investigations on single molecules using the Scanning Tunnelling Spectroscopy (STS) mode.[3,138–140] In this mode the tip is 'frozen' at a well specified distance from the sample surface (position) and dI/dU is sampled as a function of voltage (U) (in a selected range, typically within −2 and +2 V). The resulting characteristic $(dI/dU) = f(U)$ can usually be interpreted in terms of the electronic density of states.[141] Several studies on organic layers have been accomplished in UHV and at solid–liquid interfaces. The major difficulties in experiments of this type are related to sample instabilities during the measurements. For the case of UHV, studies on single copper phthalocyanines (CuPcs) by Gimzewski *et al.*[138] and later by Dekker *et al.*[142] revealed asymmetric $I(U)$ traces, namely an enhanced current at negative sample bias, attributed to a resonant tunnelling through the HOMO of the CuPc. However, the HOMO–LUMO gap of the Pc was not observed. Likewise, studies on vanadyl derivatised Pcs on Au(111) have shown strongly asymmetric $I(U)$ curves because of an enhanced tunnelling current at positive sample bias.[143,144] In this case the tunnelling occurred through the LUMO. STS explorations have also been carried out as a function of the distance between tip and surface on chemisorbed monolayers of α,α′-xylyl dithiol (XYL) on Au.[145] Increasing the tip–surface distance, the $I(U)$ curves become asymmetric. On the same molecular systems, investigations were performed tethering nanometer-sized gold clusters, deposited from a cluster beam, between the head groups of the SAM and the STM tip. UHV-STM was employed both to image these nanostructures and to measure their $I(U)$ characteristics as a function of the separation between the probe tip and the metal cluster. At room temperature, a "Coulomb staircase" behaviour was recorded. This result is in good agreement with semi classical predictions for correlated single-electron tunnelling and permits an estimation of the electrical resistance of a single XYL molecule which amounts to (18 ± 12) MΩ.[146] Similar results have been obtained on crystalline monolayers of coronene grown by sublimation on HOPG in UHV.[147] The HOMO–LUMO gap, although being smaller than the calculated value for an isolated molecule, increases with the size of the tip–sample gap.

Recently Wei and Reifenberg have shown by STS that a self-assembled monolayer of dodecanethiols on Au(111) possesses insulating electrical properties comparable to that of a 1.5 nm layer of SiO_2 on Si, suggesting its possible use as electrical insulators in future device applications.[148] Employing a different tactic, Gimzewski and Joachim have translated, in UHV with the STM tip, polycyclic aromatic hydrocarbons (PAHs) to a double atomic step of the Cu(100) surface. This step was employed as an electrode, while the STM tip behaved as a counter-electrode. In this manner the electrical properties of the single molecules through the 'conjugated diving board' was determined, revealing an exponential decay of the conductivity with the distance from the contact end.[109] The combination of STS and optical absorption measurements was used to determine the exciton binding of PPV and poly-fluorene derivatives.[149] By means of STS one can also evaluate the band gap for a conjugated polymer film of PPV. The data obtained fit well with optical spectroscopy measurements.[150] Exploiting STS and ultraviolet photoelectron spectroscopy (UPS) on unsubstituted hexa-*peri*-hexabenzocoronenes (HBCs) sublimed in UHV on Au(111), comparable results for the electronic structure of the occupied states have been sampled. Also in this case, the measured band gap is in accordance with that determined by optical absorption.[151]

Only a few STS studies have been reported on organic molecules at the liquid–solid interface. The use of STS under these conditions was introduced first by Rabe and co-workers comparing the STS plots of the saturated and unsaturated moieties in a single alkylated HBC physisorbed at the graphite–solution interface. While the $I(U)$ characteristics of the aliphatic side-chains turned out to be symmetric, those of the conjugated core moieties were asymmetric.[139] Under the same solid–liquid interface conditions, metallo-porphyrin derivatives assembled on gold surfaces have been investigated with STS. Asymmetric $I(U)$ spectra have also been found due to an increase in tunnelling current at high negative sample bias. This increase was explained by tunnelling *via* the oxidised states of the molecule.[152] Again, asymmetric traces have been recorded on self-assembled monolayers of thiol-functionalised aromatic moieties in air.[153] The molecules have been found to act as potential barriers to electron transmission.[153] The barrier is trapezoidal when the molecule has a permanent dipole moment (normal to the basal plane of the Au surface), in accordance with the asymmetric $I(U)$ traces.[154] Very recently, rectifying behaviour was probed on tetrathiafulvalene (TTF) nanostructures at the solid–liquid interface. This asymmetry in the $I(U)$ spectra was found to be strongly correlated with the

oxidation potential of the molecule, but independent on its molecular ordering.[155]

STM imaging can also provide information on the conductivity of organized architectures. The average resistances of self-assembled monolayers of linear alkanethiols with different length chemisorbed nearly perpendicular on Ag(111) was determined from the range of tunnelling parameters (tip voltage and average tunnelling current) that allowed attainment of molecularly resolved STM imaging of the head of the molecules self-assembled at surfaces. This revealed an exponential increase in the resistance of the layer with increasing length of the alkyl chain from C_2H_5SH to $C_{11}H_{23}SH$.[156]

Later, conjugated oligomers of phenylene-ethynylenes were embedded into a dodecanethiol self-assembled monolayers on Au(111). STM and microwave frequency alternating current STM at high tunnel junction impedance (100 GΩ) were used to assess their electrical properties. The inserted conjugated molecules formed single molecular wires that extended from the Au(111) substrate to about 7 Å above and were found to possess a very high conductivity as compared with that of the alkanethiolate.[157]

Dynamic electronic processes could be also detected by STM. A stochastic on–off conductivity switching in phenylene-ethynylene oligomers embedded in a SAM of alkanethiols was observed and explained in terms of changes in ring conformations, or electron localisation, or both.[158] Later, the stochastic on–off switching was monitored also on much simpler chemical systems including octanedithiol, decanedithiol, and dodecanedithiol bonded on Au(111). The rate of switching increased substantially at 60 °C, the temperature at which these films are commonly annealed. Because such switching in alkanethiols is unlikely to be determined by intra-molecular electronic changes and cannot be fully accounted for by breaking of the top contact, it was suggested that the cause is the well-known mobility of molecules tethered to gold *via* a thiol linkage, leading to a stochastic breaking of the bottom molecule metal contact.[159]

The STM based set-ups permit explorations at the single molecular level on the electrical properties of single molecules in supramolecular arrangements as well as to obtain insight into dynamic processes at the interface. These latter are crucial for the tailoring of hybrid metal–organic contacts.

Electrical measurements with Scanning Force Microscopy

A great deal of work was performed by Frisbie and co-workers using conducting probe SFM (CPSFM) to record $I(U)$ characteristics on samples that are highly resistive or surrounded by insulating regions which could then not be investigated by STM. Another difference from STM measurements, is the position of the tip. In CPSFM the tip is placed in direct contact, under controlled load, with the material to be probed. In fact the measured $I(U)$ relationship is known to be profoundly influenced by the electronic properties of the tip–sample contact. In contrast, an STM tip is generally not in physical contact with the sample, so the determined $I(U)$ characteristics suffer from the hardly reproducible tip–sample contact. While reliance of STM on tunnelling allows a powerful conductance spectroscopy that maps the electronic density of states of a material, the length scale over which one can probe transport in resistive materials is limited to typical tunnelling distances (1–10 nm).[160] Moreover the visualisation of the organic materials with SFM can be performed using the metal coated tip operating in Tapping Mode, limiting the invasivity of the imaging.

CPSFM was used to measure the electrical transport characteristics of 2–14 nm thick doped crystallites of the organic semiconductor sexithiophene (6T) sublimed in vacuum on Au and SiO_2 substrates. SFM imaging accounted for an orientation of the 6T molecules with their long axes nearly perpendicular to the substrate. While for the crystals supported on Au the transport is probed through the thickness of the crystals (*i.e.*, the vertical direction) with the CPSFM tip, on SiO_2 the transport is measured parallel to the substrate between the CPSFM tip and a nanofabricated Au electrode in contact with the crystallite. On Au a greater conductance was found for the three 6T layers rather than for the single layer thick one, suggesting that an important role is played by interchain hopping. Both the vertical and horizontal conductance measurements showed non-ohmic behavior.[161] CPSFM permits also to study the conductivity of a 6T crystal on SiO_2 at different distances from the microfabricated Au wire contact. At a given tip voltage, the current decreased with increasing distance of the probe from the wire.[160]

CPSFM can also be exploited to address the transport investigation on an individual grain boundary (GB) in a 6T crystal on a SiO_2/Si surface. A variable channel length transistor was constructed using a microfabricated Au electrode contacting one grain, an Au-coated AFM tip as a positionable electrode, and the doped Si substrate as a gate. The GB resistance was found to be gate voltage dependent and large, on the order of 10^9–10^{10} Ω for a 1 μm boundary length. Resistances across single 6T grains were an order of magnitude lower. The results indicate that GBs can be the principal bottleneck to charge transport in polycrystalline organic semiconductor films, particularly at low gate fields.[162] This was also confirmed by electrostatic force microscopy studies of the potential drop along monolayer thick hundred nanometer wide domains of a poly-thiophene, doped with $AuCl_3$.[163]

A similar experiment to that performed by STM by Heinz and Rabe on the conductivity of SAMs of alkanethiols as a function of the number of methylene units in the alkane chains packed on a metallic substrate[156] was carried out by CP-SFM using Au as support. The resistance was again found to increase exponentially with monolayer thickness. The parameter β, being the decay constant of the transconductance (G), where $G = \beta e^{-\beta l}$, with l = the length of the wire, was determined as $\beta = 1.45$ per methylene unit.[164] This value is in reasonable agreement with the ones previously reported by different authors.[165–167] The comparison of CPSFM measurements on SAMs of unsaturated oligo-phenylene thiolates and saturated alkanethiolates assembled on Au substrates revealed average β values of (0.42 ± 0.07) Å^{-1} and (0.94 ± 0.06) Å^{-1}, respectively.[168] A recent study demonstrated that important roles are played by the work function of the chosen metal electrodes and by the anchoring groups that interact with the contact.[169] The tip–SAM contact exploiting the CPSFM approach is approximately 15 nm^2.[170]

Using a Au nanocluster with a 1.5 nm diameter embedded between the conductive SFM probe and the SAM one can reduce such a size notably. The resistance of a single $HS(CH_2)_8SH$ molecule covalently linked to this Au nanocluster was measured to be (900 ± 50) MΩ. In contrast, non-bonded contacts to $CH_3(CH_2)_7SH$ monolayers were at least four orders of magnitude more resistive. Moreover these experiments were less reproducible, and had a different voltage dependence, demonstrating that the measurement of intrinsic molecular properties requires chemically bonded contacts. The conductivities determined employing the Au nanocluster fit well with first principles simulations based on tunnelling transport.[171] Reasonably, the same approach on a single carotenedithiol molecules with a total length of 28 carbons revealed a notably higher conductivity of the conjugated molecule if compared to a linear saturated alkane having an equivalent length chemisorbed on Au.[159]

Therefore CPSFM is perfectly suitable to elucidate the electrical properties of materials across a wide range of length scale on a variety of samples. Noteworthy, the use of Au nanoclusters interfaced to the conductive SFM tip as counter

electrode represents a very elegant way to wire reproducibly a small amount of molecules.

Discussion and future challenges

SPMs have indisputably widened the scope for addressing and controlling the properties of single molecules. The first scientist who dared to think so small was Richard Feynman in 1959, who, in his celebrated lecture entitled *There's Plenty of Room at the Bottom*[172] said: 'I can hardly doubt that when we have some control of the arrangement of things on a small scale we will get an enormously greater range of possible properties that substances can have, and of different things that we can do'. Different important issues still need to be tackled to improve the capability of tuning the physico-chemical properties of single molecules as well as of their ordered multi-molecular arrangements. A great challenge is the elucidation of more and more complex entities and processes. Marrying SPM studies beyond imaging with external stimuli (light, pH, applied voltage) one can explore many physico-chemical phenomena in both artificial and natural systems. The exploitation of the tip as stimuli for nanopatterning and nanomanipulation can benefit a lot from the use of different SPMs and from the development of new modes. For example Scanning Near Field Optical Microscopy[173] can be successfully used to trigger chemical reactions,[174,175] such as a polymerisation leading to a nanopatterning of the surfaces with an array of a given conjugated polymer.[176]

Concluding remarks

Scanning Probe Microscopies are demonstrated to be unique tools for casting light onto different physico-chemical properties of single molecules and on their supramolecular arrangements as well as for the nanoengineering of complex hybrid architectures at surfaces. Their versatility and simplicity in the different modes as well as their applicability to different kinds of samples provide direct access to new realms at the interface between different disciplines including chemistry, physics and biology, and open up a vast range of applications that foster materials science into the nanoscale world.

Acknowledgements

Support from the ESF-SONS-BIONICS project is gratefully acknowledged. I wish to thank Prof. Dr. Jürgen P. Rabe (Berlin) for his exceptional scientific guidance during the years I spent in his group as well as for introducing me to the astonishing realm of scanning probe microscopies and to their exploitation for insights into physico-chemical properties of nano functional materials. I also would like to express my gratitude to long-term collaborators: Prof. Klaus Müllen and Dr. Mark Watson (Mainz), Prof. Roeland J. M. Nolte and Dr. Alan E. Rowan (Nijmegen), Profs. Giovanni Gottarelli and Gian Piero Spada (Bologna), Dr. Franco Cacialli (London) and Prof. Giovanni Marletta (Catania). I thank Pieter de Witte for his comments on the manuscript.

References

1 G. Binnig, H. Rohrer, C. Gerber and E. Weibel, *Helv. Phys. Acta*, 1982, **55**, 726.
2 G. Binnig, H. Rohrer, C. Gerber and E. Weibel, *Appl. Phys. Lett.*, 1982, **40**, 178.
3 R. Wiesendanger, *Scanning Probe Microscopy and Spectroscopy, Methods and Applications*, Cambridge University Press, Cambridge, 1998.
4 G. Binnig, C. F. Quate and C. Gerber, *Phys. Rev. Lett.*, 1986, **56**, 930.
5 D. Rugar and P. Hansma, *Phys. Today*, 1990, **43**, 23.
6 C. Bustamante and D. Keller, *Phys. Today*, 1995, **48**, 32.
7 J. Tamayo and R. Garcia, *Langmuir*, 1996, **12**, 4430.
8 J. P. Rabe and S. Buchholz, *Science*, 1991, **253**, 424.
9 J. I. Paredes, A. Martínez-Alonso and J. M. D. Tascón, *Microporous Mesoporous Mater.*, 2003, **65**, 93.
10 M. M. S. Abdel-Mottaleb, S. De Feyter, A. Gesquière, M. Sieffert, M. Klapper, K. Müllen and F. C. De Schryver, *Nano Lett.*, 2001, **1**, 353.
11 R. Heinz, A. Stabel, J. P. Rabe, G. Wegner, F. C. De Schryver, D. Corens, W. Dahaen and C. Sueling, *Angew. Chem., Int. Ed. Engl.*, 1994, **33**, 2080.
12 A. Stabel, R. Heinz, F. C. De Schryver and J. P. Rabe, *J. Phys. Chem.*, 1995, **99**, 505.
13 J.-P. Bucher, L. Santesson and K. Kern, *Langmuir*, 1994, **10**, 979.
14 P. G. Vekilov and J. I. D. Alexander, *Chem. Rev.*, 2000, **100**, 2061.
15 J. K. Gimzewski and R. Möller, *Phys. Rev. B*, 1987, **36**, 1284.
16 P. K. Hansma and J. Tersoff, *J. Appl. Phys.*, 1987, **61**, R1.
17 B. Venkataraman, G. W. Flynn, J. L. Wilbur, J. P. Folkers and G. M. Whitesides, *J. Phys. Chem.*, 1995, **99**, 8684.
18 D. M. Cyr, B. Venkataraman, G. W. Flynn, A. Black and G. M. Whitesides, *J. Phys. Chem.*, 1996, **100**, 13747.
19 C. L. Claypool, F. Faglioni, W. A. Goddard, H. B. Gray, N. S. Lewis and R. A. Marcus, *J. Phys. Chem. B*, 1997, **101**, 5978.
20 R. Lazzaroni, A. Calderone, J. L. Brédas and J. P. Rabe, *J. Chem. Phys.*, 1997, **107**, 99.
21 P. Sautet, *Chem. Rev.*, 1997, **97**, 1097.
22 F. Biscarini, C. Bustamante and V. M. Kenkre, *Phys. Rev. B: Condens. Matter.*, 1995, **51**, 11089.
23 G. Orlandi, A. Troisi and F. Zerbetto, *J. Am. Chem. Soc.*, 1999, **121**, 5392.
24 A. Yajima and M. Tsukada, *Surf. Sci.*, 1996, **366**, L715.
25 J. Crystal, L. Y. Zhang, R. A. Friesner and G. W. Flynn, *J. Phys. Chem. A*, 2002, **106**, 1802.
26 P. Samorì, A. Fechtenkötter, F. Jäckel, T. Böhme, K. Müllen and J. P. Rabe, *J. Am. Chem. Soc.*, 2001, **123**, 11462.
27 P. Samorì, N. Severin, C. D. Simpson, K. Müllen and J. P. Rabe, *J. Am. Chem. Soc.*, 2002, **124**, 9454.
28 T. A. Jung, R. R. Schlittler and J. K. Gimzewski, *Nature*, 1997, **386**, 696.
29 G. V. Nazin, X. H. Qiu and W. Ho, *Science*, 2003, **302**, 77.
30 D. Cahen and G. Hodes, *Adv. Mater.*, 2002, **14**, 789.
31 A. C. Kummel, *Science*, 2003, **302**, 69.
32 G. C. McGonigal, R. H. Bernhardt and D. J. Thomson, *Appl. Phys. Lett.*, 1990, **57**, 28.
33 D. M. Cyr, B. Venkataraman and G. W. Flynn, *Chem. Mater.*, 1996, **8**, 1600.
34 X. H. Qiu, C. Wang, Q. D. Zeng, B. Xu, S. X. Yin, H. N. Wang, S. D. Xu and C. L. Bai, *J. Am. Chem. Soc.*, 2000, **122**, 5550.
35 A. Gesquière, M. M. S. Abdel-Mottaleb, S. De Feyter, F. C. De Schryver, F. Schoonbeek, J. van Esch, R. M. Kellogg, B. L. Feringa, A. Calderone, R. Lazzaroni and J. L. Brédas, *Langmuir*, 2000, **16**, 10385.
36 S. Isoda, T. Nemoto, E. Fujiwara, Y. Adachi and T. Kobayashi, *J. Cryst. Growth*, 2001, **229**, 574.
37 P. Samorì, N. Severin, K. Müllen and J. P. Rabe, *Adv. Mater.*, 2000, **12**, 579.
38 S. De Feyter and F. C. De Schryver, *Chem. Soc. Rev.*, 2003, **32**, 139.
39 C. D. Frisbie, L. F. Rozsnyai, A. Noy, M. S. Wrighton and C. M. Lieber, *Science*, 1994, **265**, 2071.
40 A. Noy, C. D. Frisbie, L. F. Rozsnyai, M. S. Wrighton and C. M. Lieber, *J. Am. Chem. Soc.*, 1995, **117**, 7943.
41 T. Han, J. M. Williams and T. P. Beebe, Jr., *Anal. Chim. Acta*, 1995, **307**, 365.
42 S. K. Sinniah, A. B. Steel, C. J. Miller and J. E. Reutt-Robey, *J. Am. Chem. Soc.*, 1996, **118**, 8925.
43 D. V. Vezenov, A. Noy, L. F. Rozsnyai and C. M. Lieber, *J. Am. Chem. Soc.*, 1997, **119**, 2006.
44 H. Zhang, H. X. He, J. Wang, T. Mu and Z. F. Liu, *Appl. Phys. A: Mater. Sci. Process.*, 1998, **66**, S269.
45 H. Schonherr, M. W. J. Beulen, J. Bugler, J. Huskens, F. van Veggel, D. N. Reinhoudt and G. J. Vancso, *J. Am. Chem. Soc.*, 2000, **122**, 4963.
46 T. Nakagawa, K. Ogawa, T. Kurumizawa and S. Ozaki, *Jpn. J. Appl. Phys., Part 2*, 1993, **32**, L294.
47 T. Nakagawa, K. Ogawa and T. Kurumizawa, *J. Vac. Sci. Technol., B*, 1994, **12**, 2215.
48 J.-B. D. Green, M. T. McDermott, M. D. Porter and L. M. Siperko, *J. Phys. Chem.*, 1995, **99**, 10965.

49 J.-B. D. Green, M. T. McDermott and M. D. Porter, *J. Phys. Chem.*, 1996, **100**, 13342.
50 R. C. Thomas, P. Tangyunyong, J. E. Houston, T. A. Michalske and R. M. Crooks, *J. Phys. Chem.*, 1994, **98**, 4493.
51 H. Skulason and C. D. Frisbie, *Langmuir*, 2000, **16**, 6294.
52 P. D. Ashby, L. W. Chen and C. M. Lieber, *J. Am. Chem. Soc.*, 2000, **122**, 9467.
53 S. Akari, D. Horn, H. Kellar and W. Schrepp, *Adv. Mater.*, 1995, **7**, 549.
54 M. G. Heaton, C. B. Prater and K. J. Kjoller, *Adv. Mater. Process.*, 1996, **149**, 27.
55 H. Skulason and C. D. Frisbie, *J. Am. Chem. Soc.*, 2002, **124**, 15125.
56 G. Papastavrou, S. Akari and H. Möhwald, *Europhys. Lett.*, 2000, **52**, 551.
57 E. W. van der Vegte and G. Hadziioannou, *Langmuir*, 1997, **13**, 4357.
58 H. Schönherr, Z. Hruska and G. J. Vancso, *Macromolecules*, 2000, **33**, 4532.
59 S. Kado and K. Kimura, *J. Am. Chem. Soc.*, 2003, **125**, 4560.
60 R. McKendry, M. E. Theoclitou, T. Rayment and C. Abell, *Nature*, 1998, **391**, 566.
61 Y. S. Leng and S. Y. Jiang, *J. Am. Chem. Soc.*, 2002, **124**, 11764.
62 D. L. Patrick, J. F. Flanagan, P. Kohl and R. M. Lynden-Bell, *J. Am. Chem. Soc.*, 2003, **125**, 6762.
63 J. Fritz, M. K. Baller, H. P. Lang, H. Rothuizen, P. Vettiger, E. Meyer, H. J. Güntherodt, C. Gerber and J. K. Gimzewski, *Science*, 2000, **288**, 316.
64 R. McKendry, J. Y. Zhang, Y. Arntz, T. Strunz, M. Hegner, H. P. Lang, M. K. Baller, U. Certa, E. Meyer, H. J. Güntherodt and C. Gerber, *Proc. Natl. Acad. Sci. U. S. A.*, 2002, **99**, 9783.
65 P. Samorì, V. Francke, K. Müllen and J. P. Rabe, *Chem. Eur. J.*, 1999, **5**, 2312.
66 S. S. Sheiko, M. da Silva, D. Shirvaniants, I. LaRue, S. Prokhorova, M. Möller, K. Beers and K. Matyjaszewski, *J. Am. Chem. Soc.*, 2003, **125**, 6725.
67 S. S. Sheiko and M. Möller, *Chem. Rev.*, 2001, **101**, 4099.
68 A. D. Schlüter and J. P. Rabe, *Angew. Chem., Int. Ed.*, 2000, **39**, 864.
69 H. Zhang, P. C. M. Grim, P. Foubert, T. Vosch, P. Vanoppen, U. M. Wiesler, A. J. Berresheim, K. Müllen and F. C. De Schryver, *Langmuir*, 2000, **16**, 9009.
70 A. Schenning, A. F. M. Kilbinger, F. Biscarini, M. Cavallini, H. J. Cooper, P. J. Derrick, W. J. Feast, R. Lazzaroni, P. Leclere, L. A. McDonell, E. W. Meijer and S. C. J. Meskers, *J. Am. Chem. Soc.*, 2002, **124**, 1269.
71 C. Rivetti, M. Guthold and C. Bustamante, *J. Mol. Biol.*, 1996, **264**, 919.
72 H. Takano, J. R. Kenseth, S. S. Wong, J. C. O'Brien and M. D. Porter, *Chem. Rev.*, 1999, **99**, 2845.
73 P. Samorì, C. Ecker, I. Gossl, P. A. J. de Witte, J. Cornelissen, G. A. Metselaar, M. B. J. Otten, A. E. Rowan, R. J. M. Nolte and J. P. Rabe, *Macromolecules*, 2002, **35**, 5290.
74 M. M. Green, R. A. Gross, F. Schilling, K. Zero and C. Crosby, *Macromolecules*, 1988, **21**, 1839.
75 J. Cornelissen, J. Donners, R. de Gelder, W. S. Graswinckel, G. A. Metselaar, A. E. Rowan, N. A. J. M. Sommerdijk and R. J. M. Nolte, *Science*, 2001, **293**, 676.
76 S. Kopp-Marsaudon, P. Leclere, F. Dubourg, R. Lazzaroni and J. P. Aime, *Langmuir*, 2000, **16**, 8432.
77 P. Leclere, F. Dubourg, S. Kopp-Marsaudon, J. L. Bredas, R. Lazzaroni and J. P. Aime, *Appl. Surf. Sci.*, 2002, **188**, 524.
78 F. Dubourg, S. Kopp-Marsaudon, P. Leclere, R. Lazzaroni and J. P. Aime, *Eur. Phys. J. E*, 2001, **6**, 387.
79 A. RosaZeiser, E. Weilandt, S. Hild and O. Marti, *Meas. Sci. Technol.*, 1997, **8**, 1333.
80 A. J. Berresheim, M. Müller and K. Müllen, *Chem. Rev.*, 1999, **99**, 1747.
81 H. Zhang, P. C. M. Grim, T. Vosch, U. M. Wiesler, A. J. Berresheim, K. Müllen and F. C. De Schryver, *Langmuir*, 2000, **16**, 9294.
82 M. Zhu, S. Akari and H. Möhwald, *Nano Lett.*, 2001, **1**, 569.
83 D. B. Grandy, D. J. Hourston, D. M. Price, M. Reading, G. G. Silva, M. Song and P. A. Sykes, *Macromolecules*, 2000, **33**, 9348.
84 T. E. Fisher, A. F. Oberhauser, M. Carrion-Vazquez, P. E. Marszalek and J. M. Fernandez, *Trends Biochem. Sci.*, 1999, **24**, 379.
85 M. B. Viani, T. E. Schäffer, A. Chand, M. Rief, H. E. Gaub and P. K. Hansma, *J. Appl. Phys.*, 1999, **86**, 2258.
86 E. L. Florin, V. T. Moy and H. E. Gaub, *Science*, 1994, **264**, 415.
87 G. U. Lee, D. A. Kidwell and R. J. Colton, *Langmuir*, 1994, **10**, 354.
88 M. Rief, H. Clausen-Schaumann and H. E. Gaub, *Nat. Struct. Biol.*, 1999, **6**, 346.
89 C. Albrecht, K. Blank, M. Lalic-Multhaler, S. Hirler, T. Mai, I. Gilbert, S. Schiffmann, T. Bayer, H. Clausen-Schaumann and H. E. Gaub, *Science*, 2003, **301**, 367.
90 M. Rief, F. Oesterhelt, B. Heymann and H. E. Gaub, *Science*, 1997, **275**, 1295.
91 M. Grandbois, M. Beyer, M. Rief, H. Clausen-Schaumann and H. E. Gaub, *Science*, 1999, **283**, 1727.
92 F. Oesterhelt, D. Oesterhelt, M. Pfeiffer, A. Engel, H. E. Gaub and D. J. Muller, *Science*, 2000, **288**, 143.
93 A. Y. Grosberg and A. R. Khokhlov, *Statistical Physics of Macromolecules*, AIP Press, New York, 1994.
94 C. Bustamante, J. F. Marko, E. D. Siggia and S. Smith, *Science*, 1994, **265**, 1599.
95 M. Rief, M. Gautel, F. Oesterhelt, J. M. Fernandez and H. E. Gaub, *Science*, 1997, **276**, 1109.
96 R. B. Best and J. Clarke, *Chem. Commun.*, 2002, 183.
97 S. Zepeda, Y. Yeh and A. Noy, *Langmuir*, 2003, **19**, 1457.
98 B. Samorì, *Chem. Eur. J.*, 2000, **6**, 4249.
99 J. Liphardt, S. Dumont, S. B. Smith, I. Tinoco and C. Bustamante, *Science*, 2002, **296**, 1832.
100 C. Bustamante, J. C. Macosko and G. J. L. Wuite, *Nat. Rev. Mol. Cell Biol.*, 2000, **1**, 130.
101 T. Hugel, N. B. Holland, A. Cattani, L. Moroder, M. Seitz and H. E. Gaub, *Science*, 2002, **296**, 1103.
102 M. F. Crommie, C. P. Lutz and D. M. Eigler, *Science*, 1993, **262**, 218.
103 T. A. Jung, R. R. Schlittler, J. K. Gimzewski, H. Tang and C. Joachim, *Science*, 1996, **271**, 181.
104 M. T. Cuberes, R. R. Schlittler and J. K. Gimzewski, *Appl. Phys. Lett.*, 1996, **69**, 3016.
105 J. K. Gimzewski and C. Joachim, *Science*, 1999, **283**, 1683.
106 J. K. Gimzewski, C. Joachim, R. R. Schlittler, V. Langlais, H. Tang and I. Johannsen, *Science*, 1998, **281**, 531.
107 F. Moresco, G. Meyer, K. H. Rieder, H. Tang, A. Gourdon and C. Joachim, *Phys. Rev. Lett.*, 2001, **86**, 672.
108 F. Moresco, G. Meyer, K. H. Rieder, H. Tang, A. Gourdon and C. Joachim, *Phys. Rev. Lett.*, 2001, **87**, 8302.
109 V. J. Langlais, R. R. Schlittler, H. Tang, A. Gourdon, C. Joachim and J. K. Gimzewski, *Phys. Rev. Lett.*, 1999, **83**, 2809.
110 C. Loppacher, M. Guggisberg, O. Pfeiffer, E. Meyer, M. Bammerlin, R. Luthi, R. Schlittler, J. K. Gimzewski, H. Tang and C. Joachim, *Phys. Rev. Lett.*, 2003, 90.
111 M. R. Falvo, S. Washburn, R. Superfine, M. Finch, F. P. Brooks, V. Chi and R. M. Taylor, *Biophys. J.*, 1997, **72**, 1396.
112 B. Samorì, *Angew. Chem., Int. Ed.*, 1998, **37**, 2198.
113 M. Cavallini, F. Biscarini, S. León, F. Zerbetto, G. Bottari and D. A. Leigh, *Science*, 2003, **299**, 531.
114 L. J. Shu, A. D. Schlüter, C. Ecker, N. Severin and J. P. Rabe, *Angew. Chem., Int. Ed.*, 2001, **40**, 4666.
115 J. Barner, F. Mallwitz, L. J. Shu, A. D. Schlüter and J. P. Rabe, *Angew. Chem., Int. Ed.*, 2003, **42**, 1932.
116 P. Samorì, H. Engelkamp, P. de Witte, A. E. Rowan, R. J. M. Nolte and J. P. Rabe, *Angew. Chem., Int. Ed.*, 2001, **40**, 2348.
117 P. Samorì and J. P. Rabe, *J. Phys.: Condens. Matter*, 2002, **14**, 9955.
118 R. D. Piner, J. Zhu, F. Xu, S. H. Hong and C. A. Mirkin, *Science*, 1999, **283**, 661.
119 A. Ivanisevic and C. A. Mirkin, *J. Am. Chem. Soc.*, 2001, **123**, 7887.
120 Y. Li, B. W. Maynor and J. Liu, *J. Am. Chem. Soc.*, 2001, **123**, 2105.
121 B. W. Maynor, Y. Li and J. Liu, *Langmuir*, 2001, **17**, 2575.
122 B. L. Weeks, A. Noy, A. E. Miller and J. J. De Yoreo, *Phys. Rev. Lett.*, 2002, 88.
123 S. H. Hong, J. Zhu and C. A. Mirkin, *Science*, 1999, **286**, 523.
124 S. Hong and C. A. Mirkin, *Science*, 2000, **288**, 1808.
125 K. B. Lee, S. J. Park, C. A. Mirkin, J. C. Smith and M. Mrksich, *Science*, 2002, **295**, 1702.
126 L. M. Demers, D. S. Ginger, S. J. Park, Z. Li, S. W. Chung and C. A. Mirkin, *Science*, 2002, **296**, 1836.
127 B. W. Maynor, S. F. Filocamo, M. W. Grinstaff and J. Liu, *J. Am. Chem. Soc.*, 2002, **124**, 522.
128 G. Agarwal, R. R. Naik and M. O. Stone, *J. Am. Chem. Soc.*, 2003, **125**, 7408.
129 R. Maoz, E. Frydman, S. R. Cohen and J. Sagiv, *Adv. Mater.*, 2000, **12**, 424.

130 G. Y. Liu, S. Xu and Y. L. Qian, *Acc. Chem. Res.*, 2000, **33**, 457.
131 S. Hecht, *Angew. Chem., Int. Ed.*, 2003, **42**, 24.
132 S. W. Hla, L. Bartels, G. Meyer and K. H. Rieder, *Phys. Rev. Lett.*, 2000, **85**, 2777.
133 S. W. Hla and K. H. Rieder, *Annu. Rev. Phys. Chem.*, 2003, **54**, 307.
134 P. C. M. Grim, S. De Feyter, A. Gesquière, P. Vanoppen, M. Rücker, S. Valiyaveettil, G. Moessner, K. Müllen and F. C. De Schryver, *Angew. Chem., Int. Ed.*, 1997, **36**, 2601.
135 Y. Okawa and M. Aono, *J. Chem. Phys.*, 2001, **115**, 2317.
136 Y. Okawa and M. Aono, *Nature*, 2001, **409**, 683.
137 A. Miura, S. De Feyter, M. M. S. Abdel-Mottaleb, A. Gesquière, P. C. M. Grim, G. Moessner, M. Sieffert, M. Klapper, K. Müllen and F. C. De Schryver, *Langmuir*, 2003, **19**, 6474.
138 J. K. Gimzewski, E. Stoll and R. R. Schlittler, *Surf. Sci.*, 1987, **181**, 267.
139 A. Stabel, P. Herwig, K. Müllen and J. P. Rabe, *Angew. Chem., Int. Ed. Engl.*, 1995, **34**, 1609.
140 R. M. Feenstra, *Surf. Sci.*, 1994, **299–300**, 965.
141 J. C. Slonczewski, *Phys. Rev. B*, 1989, **39**, 6995.
142 C. Dekker, S. J. Tans, B. Oberndorff, R. Meyer and L. C. Venema, *Synth. Met.*, 1997, **84**, 853.
143 D. E. Barlow and K. W. Hipps, *J. Phys. Chem. B*, 2000, **104**, 5993.
144 K. W. Hipps, D. E. Barlow and U. Mazur, *J. Phys. Chem. B*, 2000, **104**, 2444.
145 S. Datta, W. D. Tian, S. H. Hong, R. Reifenberger, J. I. Henderson and C. P. Kubiak, *Phys. Rev. Lett.*, 1997, **79**, 2530.
146 R. P. Andres, J. D. Bielefeld, J. I. Henderson, D. B. Janes, V. R. Kolagunta, C. P. Kubiak, W. J. Mahoney and R. G. Osifchin, *Science*, 1996, **273**, 1690.
147 K. Walzer, M. Sternberg and M. Hietschold, *Surf. Sci.*, 1998, **415**, 376.
148 A. P. Labonté, S. L. Tripp, R. Reifenberger and A. Wei, *J. Phys. Chem. B*, 2002, **106**, 8721.
149 S. F. Alvarado, P. F. Seidler, D. G. Lidzey and D. D. C. Bradley, *Phys. Rev. Lett.*, 1998, **81**, 1082.
150 R. Rinaldi, R. Cingolani, K. M. Jones, A. A. Baski, H. Morkoc, A. Di Carlo, J. Widany, E. Della Sala and P. Lugli, *Phys. Rev. B*, 2001, **63**, 75311.
151 H. Proehl, M. Toerker, F. Sellam, T. Fritz, K. Leo, C. Simpson and K. Müllen, *Phys. Rev. B*, 2001, **63**, 205409.
152 W. H. Han, E. N. Durantini, T. A. Moore, A. L. Moore, D. Gust, P. Rez, G. Leatherman, G. R. Seely, N. J. Tao and S. M. Lindsay, *J. Phys. Chem. B*, 1997, **101**, 10719.
153 A. I. Onipko, K. F. Berggren, Y. O. Klymenko, L. I. Malysheva, J. Rosink, L. J. Geerligs, E. van der Drift and S. Radelaar, *Phys. Rev. B*, 2000, **61**, 11118.
154 J. Rosink, M. A. Blauw, L. J. Geerligs, E. van der Drift and S. Radelaar, *Phys. Rev. B*, 2000, **62**, 10459.
155 M. M. S. Abdel-Mottaleb, E. Gomar-Nadal, S. De Feyter, M. Zdanowska, J. Veciana, C. Rovira, D. B. Amabilino and F. C. De Schryver, *Nano Lett.*, 2003, **3**, 1375.
156 R. Heinz and J. P. Rabe, *Langmuir*, 1995, **11**, 506.
157 L. A. Bumm, J. J. Arnold, M. T. Cygan, T. D. Dunbar, T. P. Burgin, L. Jones, II, D. L. Allara, J. M. Tour and P. S. Weiss, *Science*, 1996, **271**, 1705.
158 Z. J. Donhauser, B. A. Mantooth, K. F. Kelly, L. A. Bumm, J. D. Monnell, J. J. Stapleton, D. W. Price, A. M. Rawlett, D. L. Allara, J. M. Tour and P. S. Weiss, *Science*, 2001, **292**, 2303.
159 G. K. Ramachandran, T. J. Hopson, A. M. Rawlett, L. A. Nagahara, A. Primak and S. M. Lindsay, *Science*, 2003, **300**, 1413.
160 T. W. Kelley, E. L. Granstrom and C. D. Frisbie, *Adv. Mater.*, 1999, **11**, 261.
161 M. J. Loiacono, E. L. Granstrom and C. D. Frisbie, *J. Phys. Chem. B*, 1998, **102**, 1679.
162 T. W. Kelley and C. D. Frisbie, *J. Phys. Chem. B*, 2001, **105**, 4538.
163 T. Hassenkam, D. R. Greve and T. Bjornholm, *Adv. Mater.*, 2001, **13**, 631.
164 D. J. Wold and C. D. Frisbie, *J. Am. Chem. Soc.*, 2000, **122**, 2970.
165 L. A. Bumm, J. J. Arnold, T. D. Dunbar, D. L. Allara and P. S. Weiss, *J. Phys. Chem. B*, 1999, **103**, 8122.
166 K. Slowinski, R. V. Chamberlain, C. J. Miller and M. Majda, *J. Am. Chem. Soc.*, 1997, **119**, 11910.
167 J. F. Smalley, S. W. Feldberg, C. E. D. Chidsey, M. R. Linford, M. D. Newton and Y.-P. Liu, *J. Phys. Chem.*, 1995, **99**, 13141.
168 D. J. Wold, R. Haag, M. A. Rampi and C. D. Frisbie, *J. Phys. Chem. B*, 2002, **106**, 2813.
169 J. M. Beebe, V. B. Engelkes, L. L. Miller and C. D. Frisbie, *J. Am. Chem. Soc.*, 2002, **124**, 11268.
170 D. J. Wold and C. D. Frisbie, *J. Am. Chem. Soc.*, 2001, **123**, 5549.
171 X. D. Cui, A. Primak, X. Zarate, J. Tomfohr, O. F. Sankey, A. L. Moore, T. A. Moore, D. Gust, G. Harris and S. M. Lindsay, *Science*, 2001, **294**, 571.
172 R. Feynman, *Lecture at the Annual Meeting of the American Physical Society (California Institute of Technology*, Dec. 1959), 1959.
173 E. Betzig and J. K. Trautman, *Science*, 1992, **257**, 189.
174 P. K. Wei, J. H. Hsu, B. R. Hsieh and W. S. Fann, *Adv. Mater.*, 1996, **8**, 573.
175 J. A. DeAro, R. Gupta, A. J. Heeger and S. K. Buratto, *Synth. Met.*, 1999, **102**, 865.
176 R. Riehn, A. Charas, J. Morgado and F. Cacialli, *Appl. Phys. Lett.*, 2003, **82**, 526.